ACS OMEGA

Open Access

http://pubs.acs.org/journal/acsodf

Article

One Reaction: Two Types of Mechanism—SARA-ATRP and SET-LRP—for MMA Polymerization in the Presence of PVC

Edina Rusen,* Alexandra Mocanu, Oana Brincoveanu, Gabriela Toader, Raluca Gavrila, Aurel Diacon, and Cristina Stavarache

Cite This: *ACS Omega* 2024, 9, 42455−42469

Read Online

ACCESS | Metrics & More | Article Recommendations | Supporting Information

ABSTRACT: This study presents for the first time the polymerization of methyl methacrylate (MMA) in the presence of poly(vinyl chloride) (PVC) that takes place by both SARA-ATRP and SET-LRP mechanisms. The two types of polymerizations that occur in the system are PMMA grafting to the PVC backbone and the formation of a new PMMA polymer, both occurring in the presence of a Cu^0wire. The polymerizations were controlled as confirmed by the molecular weight evolution, polymerization kinetics, and variations in the dispersity value. The MMA polymerization in the presence of PVC at 60 and 70 °C leads to the formation of two polymer species characterized by an increase in the molecular weight with the conversion and a narrowing of the dispersity value with the reaction progress. To increase the degree of control over the polymerization, the same reaction was performed at room temperature, which allowed us to highlight the presence of the SARA-ATRP and SET-LRP mechanisms via subsequent polymer chain extensions. The results demonstrated that PMMA grafting on PVC polymers follows a SARA-ATRP mechanism, while the formation of a PMMA homopolymer entails a SET-LRP process. The influence of solvent nature on the polymerization reaction was studied by performing the grafting of *N*-isopropylacrylamide (NIPAM) onto the surface of PVC particles in aqueous media in the presence and in the absence of $CuCl_2$. The polymerization reactions and the obtained materials were studied by gel permeation chromatography (GPC), ^{1}H NMR, DMA, scanning electron microscopy (SEM), and atomic force microscopy (AFM).

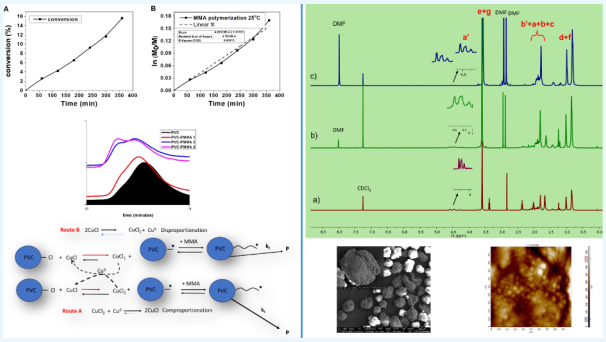

1. INTRODUCTION

Polyvinyl chloride (PVC) is one of the most used commercially available polymers due to its low production cost, its properties, such as chemical resistance to acids and base, and good compatibility with additives, such as plasticizers, thermal stabilizers, lubricants, and filler agents.[1,2] The chemical modification of PVC is usually performed through nucleophilic substitution of chlorine atoms to enhance its mechanical properties.[3,4] Reversible-deactivation radical polymerization (RDRP) techniques include precise synthesis methods to obtain macromolecular compounds with tailored architectures and accurate control over the molecular weight of polymer chains.[5−7] Controllable architectures can also be achieved by ionic polymerizations,[8] but more stringent conditions are required, making RDRP more appealing. The most widely used RDRP processes include nitroxide-mediated radical polymerization,[9,10] reversible addition−fragmentation chain transfer (RAFT),[11,12] and atom transfer radical polymerization (ATRP).[13−15]

The chemical modification of PVC to enhance certain properties can be achieved by grafting mechanisms.[16−18] Up to now, the grafting process has been achieved predominantly by three routes: "grafting onto", "grafting from", and "grafting through", resulting in the formation of different polymer architectures, such as comb- or brush-type graft copolymers. The "grafting from" approach is one of the more intensely used methods that allows the use of controlled polymerization techniques. This method can usually be employed in two types of processes: surface grafting and graft copolymerization. The surface grafting approach implies that only the surface is modified without changing the properties of the bulk. Graft copolymerization involves the reaction of a preformed homopolymer or copolymer with fresh monomers, which are then covalently bonded to the polymer chains; therefore, conventional polymerization methods can be applied.

The reversible transfer of a halogen atom to propagating radicals capable of forming dormant species represents a

Received: July 4, 2024
Revised: August 27, 2024
Accepted: September 6, 2024
Published: September 29, 2024

dominant, adaptable, and scalable alternative to attain control over macromolecular species reactivity,[15,19,20] This route is the basis of the atom transfer radical polymerization (ATRP) process. The molecular weight of a polymer resulting from the ATRP process increases linearly with the conversion while preserving a low dispersity value, which indicates that all chains extend simultaneously.[21]

Recently, our team demonstrated the grafting both on the surface and in homogeneous media of poly(acrylic acid) from PVC by the ATRP process.[17] The literature presents an impressive number of papers on ATRP processes for the chemical modification of PVC with polymers,[16,22−24] however, there is no mention of a process in the presence of metallic copper. Therefore, this study focused on the grafting of PMMA and PNIPAM in homogeneous and heterogeneous media using a metallic copper catalyst.[25,26] There is still a scientific debate regarding the polymerization mechanism.[27] Thus, Matyjaszewski's group sustains a SARA (supplemental activator and reducing agent) ATRP mechanism,[28−31] while the group of Prof. Percec sustains a SET-LRP (single electron transfer living radical polymerization) mechanism.[32−36]

The SARA ATRP and SET-LRP mechanisms use the same components and involve same reactions but they differently contribute to the overall polymerization. Both mechanisms are characterized by primary deactivation by Cu (II) and negligible deactivation by Cu (I)[37] (Scheme 1).

Scheme 1. Specific Comproportionations and Disproportionations of SARA-ATRP and SET-LRP

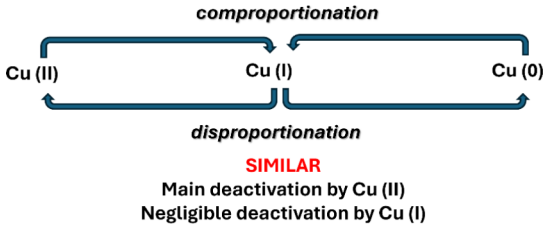

The following are the key distinctions among the proposed mechanisms:

●For SARA-ATRP, Cu^{1+} is the main activator, while Cu^0 is a supplemental sacrificial and reducing agent in comparison the SET-LRP considers Cu^0 as the activator of alkyl halide.

●For SARA-ATRP comproportionation is specific, while for SET-LRP it is disproportionation.[30]

●In the case of SARA-ATRP is limited termination versus SET-LRP, where zero termination and end group functionality is 100%.

●For SARA-ATRP, the activation step is via Inner Sphere Electron Transfer (ISET), while for SET-LRP it involves other Sphere Electron Transfer (OSET).[33]

Thus, the major difference between the two types of mechanisms consists of the proportion in which each species (Cu^0, Cu^{1+}, and Cu^{2+}) participates in the polymerization evolution. This aspect is key to determining which mechanism is favored. The type of copper ions involved in each step depends on the nature of the ligand used, which influences its solubility in the reaction medium.[38] Thus, the solubility of the complex formed by the ligand and the copper ions is critical for establishing the mechanism.

Regardless of the debate over the mechanism,[39−42] in practical applications, Cu^0 has several **key advantages** compared to other **RDRP**[40,43−48] methods, which include fast and ultrafast reaction rates at room temperature,[49−51] simple reaction setup,[37] only trace amounts of copper are retained in the final polymer,[52] nearly colorless products,[53] tolerance to impurities[54,55] and air, compatibility with a wide range of organic solvents[56,57] and aqueous media.[58,59] The presented examples are specific to homogeneous systems, although a relatively recent study[60] presented the synthesis of mini-emulsions by SARA-ATRP, thus widening the versatility of the mechanism.

The copper traces can be eliminated from the system by using "metal-free" polymerization procedures.[61−64] The disadvantage of this strategy is that it involves an organic photocatalyst, such as pyrene,[65] perylene,[66] or fenoxazine[67] derivatives, which are not entirely environmentally friendly.

The polymer properties and applications are dictated by their molecular architecture (composition, topology, and functionality), molecular weight, and dispersity value. The large-scale implementation of ATRP and RDRP has given rise to a series of potential environmental issues.[59] These are related to the toxicity of the monomer, catalysts, solvents, additives, and energy requirements. In our case, for the initiating species, we used a preformed (nontoxic) polymer and a low-toxicity monomer (methyl methacrylate).[68] Also, the catalyst, a copper wire, can be easily removed from the system after polymerization and reused. The reaction reaches high conversion values (resulting in low waste generation), and it has low energy requirements because it can be performed at room temperature. Considering the 12 principles of green chemistry, our process satisfies most of the issues. Nevertheless, the second principle (design methods to maximize the incorporation of all substrates used in the chemical process into the final product (atom economy)) requires additional study to determine the possibility of utilization of the final product as obtained or after separation and can constitute the topic of future studies related to green chemistry aspects of controlled polymerization reactions in the presence of Cu^0.

PMMA presents excellent impact and weathering resistance. Through the modification of PVC with PMMA chains, the final product will display some of the PMMA characteristics, thus increasing its mechanical resistance as well as its UV resistance; therefore, reducing the need for additional compounds (UV absorbers or other filling agents, which tend to leach in the environment) to be integrated into the final product.

The recycling of polymers is one of the main objectives of circular economy. The integration of controlled radical polymerizations for this goal can be achieved through the exploitation of the activation of the dormant polymer chain-end functionality. Controlled radical polymerizations create an avenue for polymerization and depolymerization through activation of the dormant polymer chain-end functionality. Martinez et al.[69] present that depolymerizations can be conducted in tetra(ethylene glycol) dimethyl ether with zerovalent Fe^0 as a supplemental activator and reducing agent, with conversions reaching over 70%. The monomer isolated during depolymerization is recovered by distillation. The temperature of the process was 170 °C, which did not affect the PVC backbone. The residual PVC could be recycled mechanically or thermally, as presented in the literature.[70,71]

This study presents for the first time the grafting of PMMA in homogeneous media on PVC in the presence of a Cu^0 metal catalyst and the grafting of PNIPAM on the surface of PVC

https://doi.org/10.1021/acsomega.4c06179
ACS Omega 2024, 9, 42455−42469

particles in aqueous media. The advantage of the proposed strategy lies in the fact that the reaction media is not contaminated with copper ions, but the mechanism by which the process occurs must also receive attention. Thus, the goal of this study is to both demonstrate a fast, efficient, and reliable strategy for modifying the properties of PVC and to investigate the mechanisms involved in the process by considering the characteristics of both SARA-ATRP and SET-LRP reaction pathways as presented in the literature.[41,42] The control over this polymerization appears to be dependent on several factors, including solvent type and temperature, which motivated the initial development of the reaction in bulk to obtain a more economically viable route. The present study highlights the synthesis of two species involving two reaction mechanisms during a single reaction stage. Moreover, this study highlights for the first time the coexistence of the same polymerization reaction of both the SET-LRP and SARA-ATRP mechanisms.

2. MATERIALS AND METHODS

2.1. Materials. Polyvinyl chloride PVC (Mn = 44600 g/mol, Đ = 2.4) (OLTCHIM S.A. Romania) was obtained by suspension polymerization and used as received. Methyl methacrylate (MMA) (Sigma-Aldrich) was purified by vacuum distillation under reduced pressure in a stream of Argon gas, and a center fraction was collected (bp 46 °C/100 mmHg). *N*-isopropylacrylamide (NIPAM, Aldrich, 97%) was recrystallized from hexane. Cu^0 wire with a diameter of 0.025 mm was obtained from Alfa Aesar. Tetrahydrofuran (THF) (Aldrich), *N*-methyl pyrrolidone (NMP) (Aldrich), dimethylformamide (DMF) (Aldrich), 2,2′-bipyridine (BiPy) (Aldrich), *N*,*N*,*N*′,*N*″,*N*‴-pentamethyldiethylenetriamine (PENTA) (Aldrich), CuCl (Aldrich), $CuCl_2$ (Aldrich), and methanol (Aldrich) were used as received.

2.2. Methods. *2.2.1. Polymerization of MMA in the Presence of PVC in Homogeneous Media.* In a 15 mL glass vial, 0.1 g of PVC was added followed by the addition of 10 mL of MMA. A magnetic PTFE stirring bar wrapped with 5 cm of copper wire was subsequently added to the vial in the presence of 10 mmol of PENTA. The vial was then sealed with a silicon rubber septum, followed by deoxygenation by bubbling with nitrogen for 10 min. The polymerization was allowed to occur at ambient temperatures of 60° and 70 °C and stirred at 200 rpm. Samples were taken periodically under a nitrogen blanket for gravimetric and GPC analysis. To establish conversion, the collected samples were precipitated in methanol, filtered, and dried at 70 °C under reduced pressure. The same procedure was employed for the polymerization at room temperature with the addition of 0.0003 g $CuCl_2$. The molar ratio between MMA: PVC = 62.5.

2.2.2. Chain Extension of the PVC Modified with PMMA Obtained at Point 2.2.1. The synthesis of the polymer was performed in DMF using as starting material the modified PVC obtained as described in Section 2.2.12.2.1 at a temperature of 70 °C (characterized by a bimodal molecular weight distribution (Mn_1 = 434000 g/mol, Đ = 1.27 and Mn_2 = 66780 g/mol, Đ = 1.47). Thus, 0.2 g of PVC modified with PMMA (70 °C) was dissolved in 5 mL of DMF, and 2 mL of MMA was added. The mixture was subjected to nitrogen purging, after which 0.0003 g of CuCl and 0.0005 g of BiPy were added. The reaction vial was sealed and heated at 80 °C with stirring for 2 h. Then, the reaction mixture was precipitated in methanol, filtrated, and dried under a vacuum until a constant mass was obtained.

2.2.3. Grafting of PNIPAM onto PVC Particle Surface in Aqueous Media. In a 20 mL reactor, 15 mL of distilled water was added followed by 0.1 g of PVC and 1 g of NIPAM. A magnetic stirring bar was wrapped with 5 cm of copper wire. The mixture was nitrogen purged for 10 min, followed by starting the reaction at room temperature by the addition of 10 mmol of of PENTA ligand. After 4 h reaction time, the reaction mixture was poured into 50 mL of distilled water, followed by filtration of the PNIPAM-modified PVC particles and drying at 50 °C until a constant mass was obtained. The same procedure was employed for the polymerization in the presence of 0.0003 g of $CuCl_2$.

2.3. Characterization. The molecular weights of the obtained polymers were analyzed using a PL-GPC 50 Integrated GPC/SEC System (Agilent Technologies) with a flow rate of 1 mL/min THF and a column oven temperature of 40 °C. Polystyrene was used as a standard and a refractive index detector was employed. The GPC equipment was calibrated using polystyrene standards (with molecular weights ranging from 162 to 10 000 000 g/mol across 18 points). The GPC traces were treated according to Gavrilov et al.[72]

The morphological and structural characterization was acquired with a Nova NanoSEM 630 Scanning Electron Microscope (FEI Company, Hillsboro, OR, USA) at an acceleration voltage of 10 kV and an element energy dispersive spectroscopy (EDX) system (Smart Insight AMETEK) at an acceleration voltage of 15 kV.

The NMR analyses were performed on a Bruker Advance III HD 600 MHz spectrometer (Bruker, Rheinstetten, Germany), corresponding to a resonance frequency of 600.12 MHz for the ^1H nucleus equipped with a 5 mm multinuclear direct detection z-gradient probe head (BBI). Samples were analyzed by using $CDCl_3$ as a solvent.

The DMA analyses were performed using a DMA 850 Discovery TA Instruments, single cantilever mode, oscillation mode, frequency 1 Hz, temperature ramp from 30 to 150 °C, heating rate 5 °C/min, and amplitude of oscillation 10 μm.

For imaging and mechanical measurements, specimens from each sample were prepared by sprinkling a small supply of sample powder on the substrate coated with an anchoring adhesive, succeeded by blowing off the surface to remove loosely attached particles. Optical inspection revealed a few remaining grains stuck on the substrate, tens of micrometers in size.

AFM measurements were performed on the surface of these grains using a Ntegra AFM (Nt-MDT) equipped with a closed-loop feedback system for compensating for the hysteresis and nonlinearities. Prior to mechanical measurements, images of the samples were acquired in tapping mode. Imaging and mechanical measurements were performed with DCP20 probes (Nt-MDT) with a nominal spring constant of 48 N/m, a tip radius of 100 nm, and a tip angle of 220°. AFM images revealed that grains generally consisted of large clumps of individual features (particles) hundreds of nanometers in size (bigger than the tip radius). Suitable measurement sites where constituent particles were exposed at the surface (as seen in SEM image X) were selected for further force curve spectroscopy. A number of approximately 20 force curves were collected for each specimen on spots corresponding to individual particles. The maximum Z displacement toward the surface was 100 nm in all cases. Inverse optical lever sensitivity (IOS) was established by measuring the slope of several recorded force curves on sapphire, which was taken as an

https://doi.org/10.1021/acsomega.4c06179
ACS Omega 2024, 9, 42455−42469

infinite rigidity material. Next, for fitting and analysis purposes, the force−displacement curves were converted to force−separation curves by adding the cantilever deflection to the position of the scanner during the loading process. Finally, the Hertzian fit was applied to the resulting curves to determine the E value. Data processing was assisted by Image AnalysisTM software (Nt-MDT).

3. RESULTS

3.1. Bulk MMA Polymerization in the Presence of PVC at 60 and 70 °C. ATRP is a polymerization method that allows for the fabrication of controlled polymer architectures. Besides the multiple advantages that this technique offers, it also has a major drawback, which is the contamination of the polymer with copper ions. Based on the literature examples,[38,73] some strategies avoid this contamination, but to the best of our knowledge, their application for PVC modification has not been implemented. Based on this reasoning, a strategy using Cu^0 metal was chosen for the fabrication of polymer grafts on a PVC backbone. Thus, the bulk polymerization of MMA using PVC as an initiator was performed at 60 and 70 °C. From Figure 1, it can be noticed that after the first 80 min, the process undergoes an autoacceleration (70 °C) phase, which makes detailed analysis of the process difficult and justifies the utilization of a lower temperature (60 °C) to better assess the polymerization.

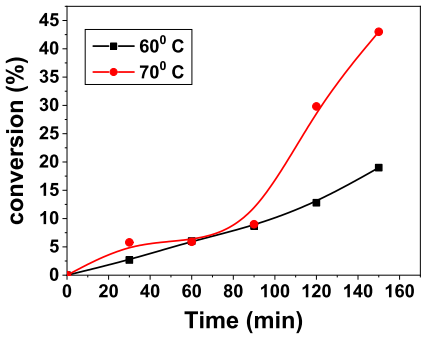

Figure 1. Conversion versus time at different reaction temperatures: 60 and 70 °C.

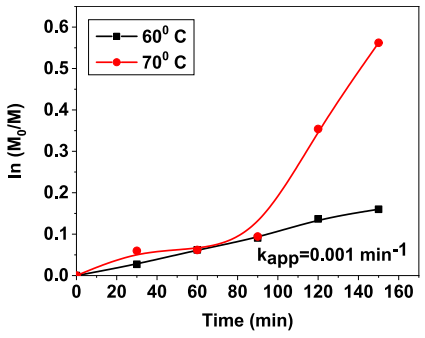

Figure 2. $\ln([M]_0/[M])$ versus time at the different reaction temperatures: 70 and 60 °C.

At a lower temperature (60 °C), the conversion versus time dependence is linear. The graphical representation of $\ln([M]_0/[M]) = f(t)$ (Figure 2) permits a preliminary assessment of the reaction progress. It is easily noticeable that the process appears to be controllable (no chain-breaking reaction),[74,75] with an apparent polymerization constant k_{app} = 0.001 min^{-1}, which is a relatively low value compared to other controlled polymerization reactions.[76,77]

Following the polymerization reactions, two polymer species (a bimodal distribution) were obtained and characterized by $\mathbf{Mn_1}$ and $\mathbf{Mn_2}$ (at 60 °C) and $\mathbf{Mn_1}$' and $\mathbf{Mn_2}$' (70 °C), possibly due to different mechanisms being present and requiring further investigation for clarification. The role of metallic Cu^0 in the catalytic system is explained within the SET-LRP process, as sustained by the Percec group,[33,36,78] and by the SARA-ATRP process as indicated by the Matyjaszewski group.[29,41,79] For a clearer understanding of the polymerization process, the variations in the two molecular weights was presented separately, **one in the order of the PVC molecular weight (10^4g/mol), while the other in the 10^6 g/mol domain**. Thus, according to Figure 3A,C, the molecular weight variation with reaction time (for $\mathbf{M_{n1}}$**−in the PVC molecular weight domain**) has the same effect for both reaction temperatures, with an initial high increase of the molecular weight followed by a slow one. In Figure 3B,D, the molecular weights of $\mathbf{M_{n2}}$ and $\mathbf{M_{n2}}$' are of **the 10^6 order** and can be explained by the formation of the PMMA homopolymer via chain transfer reactions with the monomer. In both cases, an increase in the molecular weight with reaction time can be observed.

The variation of the dispersity (Đ) value during the polymerization process is another aspect that can be used to characterize the control characteristics of the reaction. From Figure 4, it can be observed a decrease of the dispersity value from 2.4, specifically for **unmodified PVC**, to 1.5 or even 1.2. In the case of **high-molecular weight** species (Figure 4), at both reaction temperatures, an increase in the dispersity value with the reaction progress was registered from values of 1.1 to 1.3 or even 1.5. It is certain that, in the case of the $\mathbf{M_{n1}}$ and $\mathbf{M_{n1}}$' molecular weight species, monomer grafting occurs, specially PMMA on the PVC chains. In the case of $\mathbf{M_{n2}}$, $\mathbf{M_{n2}}$' species, a new polymer is generated, PMMA homopolymer. The first conclusion is that ***two polymeric species are generated through one reaction***.

Additional information can be obtained by tracking the evolution in time of the percentage of each type of polymeric species generated: the modified PVC and PMMA homopolymers for the reaction at 60 °C. This temperature was chosen because it allowed controlling the polymerization reaction. At a temperature of 70 °C the linearity is exhibited up to 90 min after which the autoacceleration phenomena are present, as confirmed by the viscosity increase of the reaction medium, the diffusion processes being favored.[80]

Each type of polymeric species generated—the modified PVC and the PMMA homopolymer for the reaction at 60 °C was determined by integrating the GPC signal (area of the peak) for the two species. Analyzing Figure 5A, it can be noticed that in the case of the **modified PVC, the percentage of polymer continuously decreases, evidently due to the formation of the PMMA homopolymer**. Using the calculated percentage of the polymers, the conversion value was also calculated (Figure 5B). The linearization of this equation (Figure 5C) is presented. Linear fitting (Figure 5C, $\mathbf{Mn_1}$**and** $\mathbf{Mn_2}$) in the case of both species demonstrated without any doubt the control characteristics of the reaction with k_{app} value of approximatively 0.00035 min^{-1} (modified PVC with PMMA) and 0.00055 min^{-1} (for the novel PMMA species).

3.2. Polymerization of MMA in the Presence of PVC at Room Temperature. To shed light on the mechanistic

https://doi.org/10.1021/acsomega.4c06179
ACS Omega 2024, 9, 42455−42469

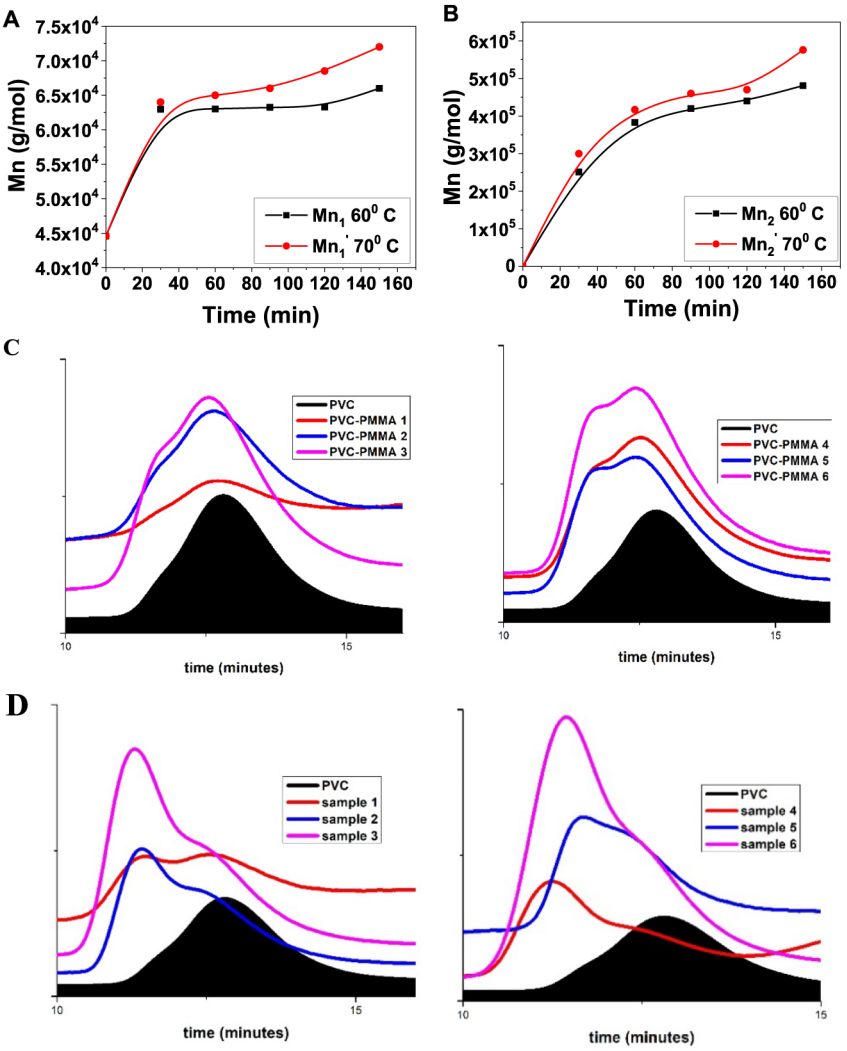

Figure 3. Variation of M_{n1}, M_{n1}' versus time (A); variation of M_{n2}, M_{n2}' versus time (B); and the GPC traces at (C) 60 °C and (D) 70 °C.

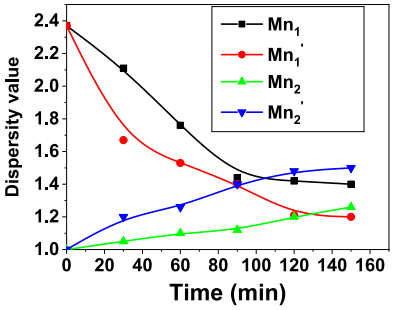

Figure 4. Variation in dispersity value for the molecular weight species M_{n1}, M_{n1}' (same order of magnitude as PVC) and M_{n2}, M_{n2}' (in the 10^6 range) versus time.

aspects of the PVC grafting method, the polymerization was also performed at 25 °C in order to reduce/eliminate the chain transfer reaction,[15] which leads to a narrowing of the dispersity value.

Figure 6A presents the variation of the conversion with the reaction time for MMA polymerization in the presence of PVC at 25 °C under identical conditions as those for the polymerizations performed at 60° and 70 °C. The variation in conversion with time is linear, which is also true for the representation of $\ln(M_0/M)$ depending on the reaction time, as shown in Figure 6B. The linear fitting allows the determination of a k_{app} value of 0.00047 min^{-1}.

As in the case of the polymerization performed at 60 °C, two types of molecular weights are obtained at the same time: one in the same order of **magnitude as the initial PVC,** which represents the polymer grafts on the PVC backbone and one of the orders of **magnitude 10^6, which represents the formation of a new polymer, probably PMMA**, generated by the chain transfer reaction with the monomer.

Figure 7B presents the variation in the dispersity value, which demonstrates that the polymerization process is controlled. In the case of the **PVC grafts, the dispersity value** decreased from 2.4 to 1.6, while **for the newly formed polymer**, the dispersity value varied from around 1.2. Using the peak area for each molecular weight from the GPC analysis, the percentage of each species was calculated, meaning the grafts and the newly formed polymer, respectively (Figure 7C). From the results, it can be observed that the percentage of modified PVC slightly decreased with time in favor of the PMMA formation in the system.

The ^{1}H NMR spectra of PVC-*g*-PMMA 1 and PVC-*g*-PMMA-2 display the following characteristic signals: the multiplet at 4.59−4.29 ppm (a') assigned to the methine

https://doi.org/10.1021/acsomega.4c06179
ACS Omega 2024, 9, 42455−42469

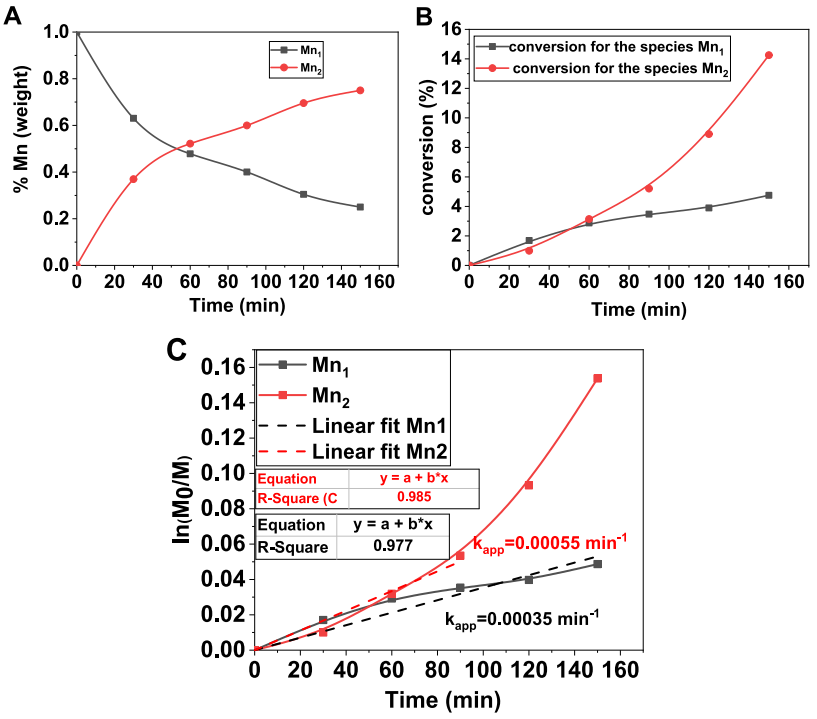

Figure 5. Variation of $\%M_{n1}$ and $\%M_{n2}$ with reaction time (A); variation of % conversion M_{n1} and M_{n2} (B); ln M_0/M versus time (C).

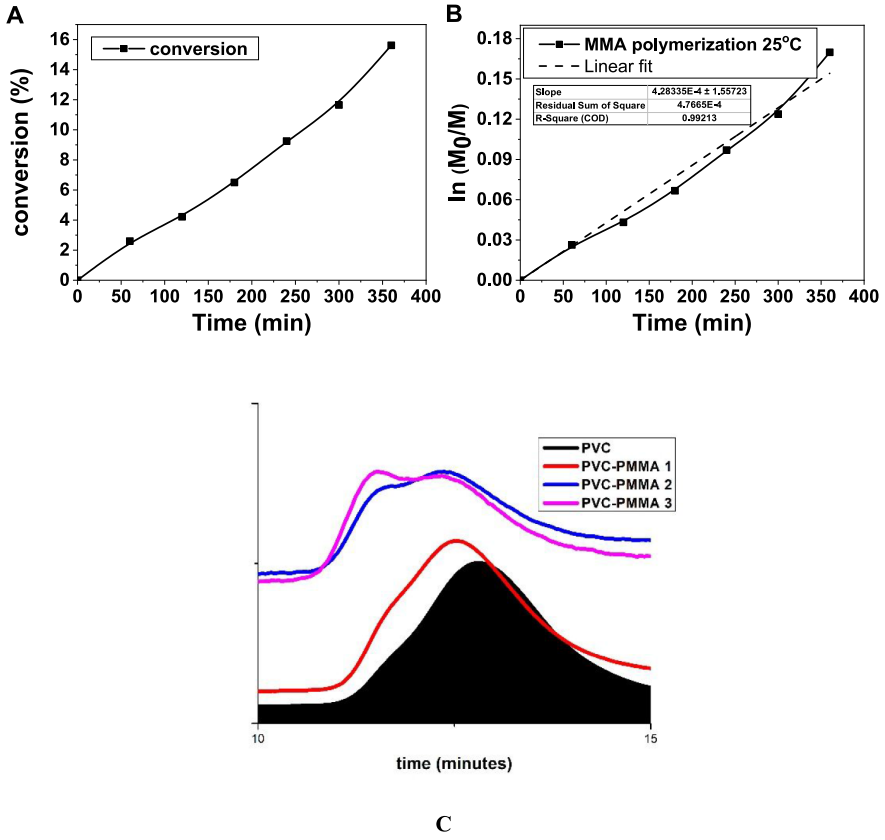

Figure 6. Variation of the conversion with time (A); ln M_0/M = f(t) (B); and GPC traces (C)

proton (−CH−Cl) of PVC; the strong singlet at 3.69 ppm corresponding to the methoxy groups ($-OCH_3$); and the 1.81 ppm signal (c) from the methylene group ($-CH_2-Cq$) of MMA units. The 2 singlets at 1.01 and 0.84 ppm are the proton resonance of the methyl group ($-CH_3$) of the PMMA chain. The other assignments (b, b', and a) are presented in Figure S1a,b and are consistent with previous literature examples.[81,82]

For the spectrum of compound PVC-*g*-PMMA-3, the same chemical shifts are observed for the signals as in the other

https://doi.org/10.1021/acsomega.4c06179
ACS Omega 2024, 9, 42455−42469

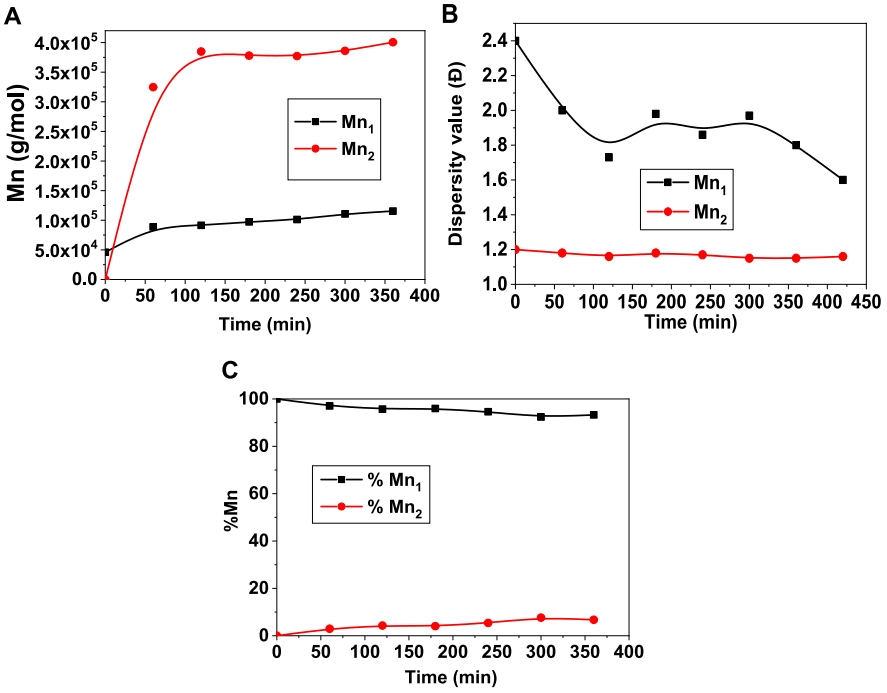

Figure 7. Variation of M_{n1} and M_{n2} (A); dispersity values for M_{n1} and M_{n2} (B); % of M_{n1} and M_{n2} with reaction time (C).

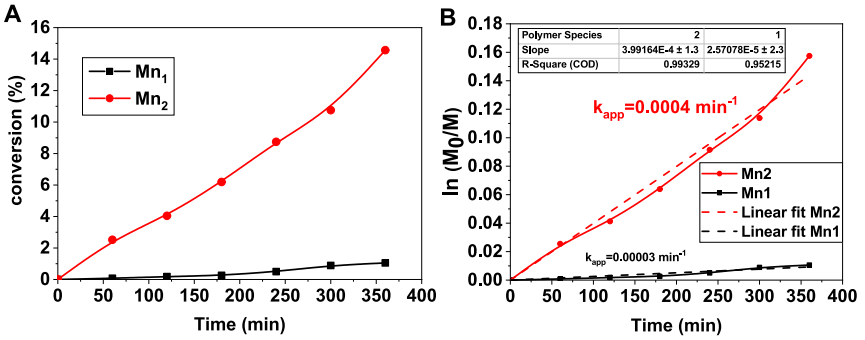

Figure 8. M_{n1}, M_{n2} conversion depending on the reaction time (A); linearization of $\ln(M_0/M) = f(t)$ for M_{n1} and M_{n2} (B).

spectra but with an increase in the intensity of the signals corresponding to the PMMA chain due to the increase of its amount used in synthesis.

From the integral values of the methoxy protons ($-OCH_3$) and of the methine proton ($-CH-Cl$), the molar ratio of the PVC:PMMA was assessed to be 1:3 in the PVC-*g*-PMMA spectra, while in the spectrum of PVC-*g*-PMMA-2, the PVC:PMMA was 1:5, and in compound PVC-*g*-PMMA-3 was 1:37.

Thus, using the ^{1}HRMN characterization method, the synthesis of graft copolymer, modified PVC. Increasing the reaction time, the molar ratio between PVC and PMMA decreased. Unfortunately, the synthesis of the homopolymer PMMA is difficult to attribute because the weight percentage provided from the mixture of PVC-*graft*-PMMA with PMMA was less than 10% weight (Figure 5).

To note the obtained PMMA homopolymer, DMA analysis was performed on the same samples used in the case of ^{1}HRMN characterization. The results are presented in Figure S2.

In the cases of the samples **PVC-*graft*-PMMA-1** and **PVC-*graft*-PMMA-2**, the values of the Tg increased compared to that of pure PVC, (80 °C), sustaining the modification of the PVC backbone. In both cases, a single Tg value is indicated, which is explained by the physical compatibility between PVC and PMMA. For the sample **PVC-*graft*-PMMA 3**, two values of Tg are noticed. This behavior could be attributed to the coexistence of the two types of polymers PVC modified with PMMA and PMMA homopolymer.

Considering the conversion at different reaction intervals, respectively, the % of each species, it is easy to determine the conversion of each type of polymer **Mn_1** and **Mn_2** (Figure 8A). Moreover, the linearization of ln M_0/M as a function of time for both species formed at the same time (Figure 8B) allows for the determination of the reaction rate (k_{app}) for each type of polymerization. It can be observed that the PMMA synthesis rate was 14 times greater than the PVC graft formation. What can be ascertained up to this point is that both reactions, **the grafting and the PMMA synthesis, are controlled polymerization process with a dispersion value relatively narrow or decrease with the reaction progress.** Considering the examples in previous literature,[40] it is relatively easy to conclude that **the grafted PMMA on the PVC polymer backbone follows a SARA-ATRP, while the PMMA synthesis follows a SET-LRP mechanism**. These conclusions are based on the fact that the SET-LRP reactions are much faster than those of SARA-ATRP.

https://doi.org/10.1021/acsomega.4c06179
ACS Omega 2024, 9, 42455−42469

Scheme 2. Two Polymerization Routes: A) SARA-ATRP and B) SET-LRP

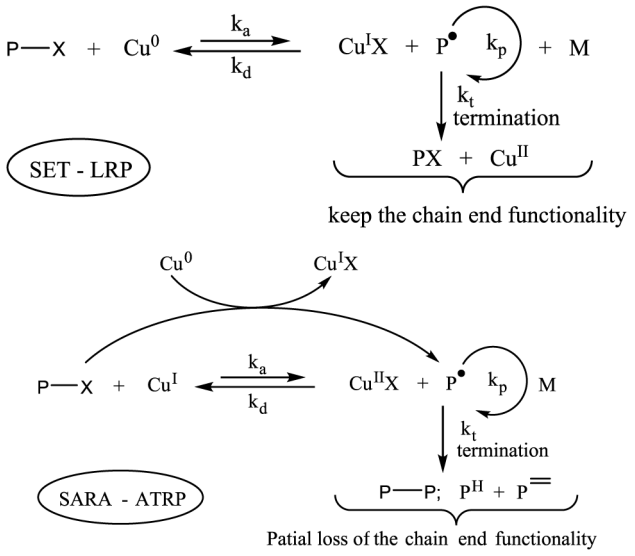

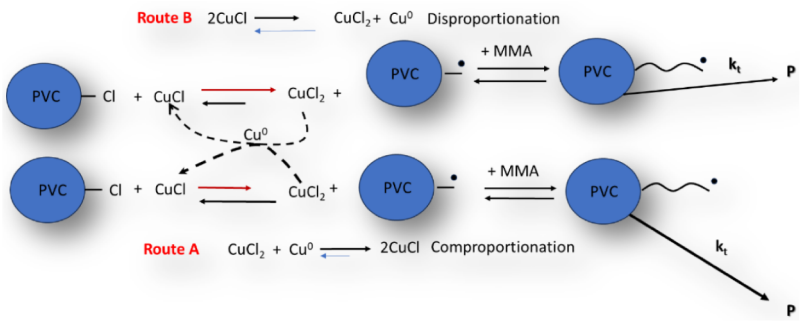

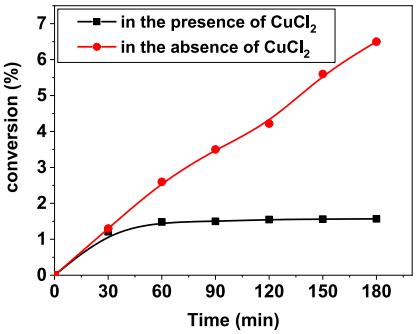

Figure 9. Conversion versus time for the MMA polymerization in the presence of PVC (bulk polymerization) (presence and absence of $CuCl_2$).

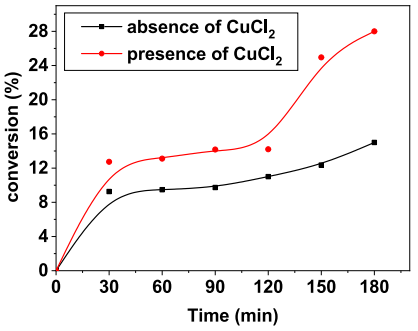

Figure 10. Conversion versus time for MMA polymerization in the presence of PVC (polymerization in NMP) (presence and absence of $CuCl_2$) (a).

The schematic representation of the possible polymer grafting routes is presented in Scheme 2 and it consists of the two controversial polymerization mechanisms SET-LRP and SARA-ATRP. The polymerizations took place through SARA-ATRP, which involved the grafting of PMMA in the PVC chain, respectively, through SET-LRP, which is the homopolymerization reaction of MMA. The two reactions are shown in Scheme 1. The termination in the case of SET-LRP is disproportionated, and the reactivity of the terminal chain is not lost, unlike in SARA-ATRP, where it is comproportionated and the partial reactivity of the chain is lost.

3.3. Bulk Polymerization of MMA in the Presence of PVC and $CuCl_2$ at Room Temperature. It has been established in the literature that in some cases, **the addition of $CuCl_2$ promotes the SARA-ATRP mechanism** .[83,84] Figure 9 presents the evolution for MMA polymerization using PVC at room temperature in the presence of $CuCl_2$, respectively, in the absence of $CuCl_2$. The analysis of Figure 9 reveals a stagnation of the reaction progress at low conversion values **in the presence of $CuCl_2$, which sustains its role as a deactivator** .[38,85]

3.4. MMA Polymerization Using PVC at Room Temperature in NMP, in the Presence of $CuCl_2$. In the case of the polymerization performed in NMP, it can be noticed that the addition of $CuCl_2$ increases the conversion

https://doi.org/10.1021/acsomega.4c06179
ACS Omega 2024, 9, 42455−42469

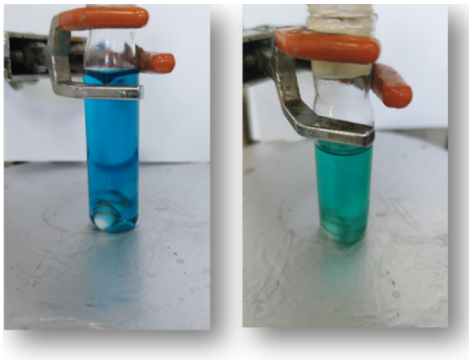

a) b)

Figure 11. Images of the $CuCl_2$ solution in NMP (a) and MMA (b) (bulk polymerization).

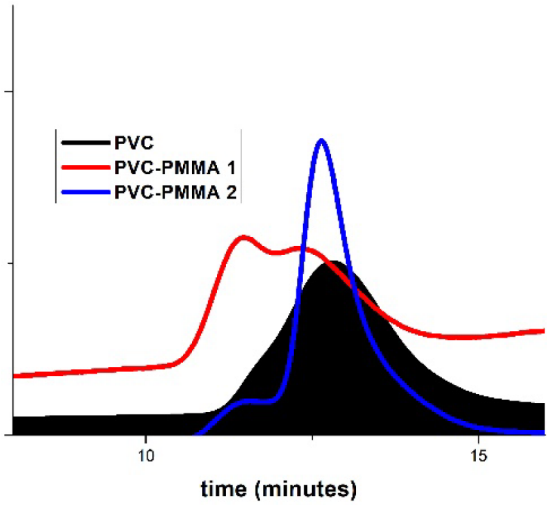

Figure 12. GPC traces for the PMMA polymer extension.

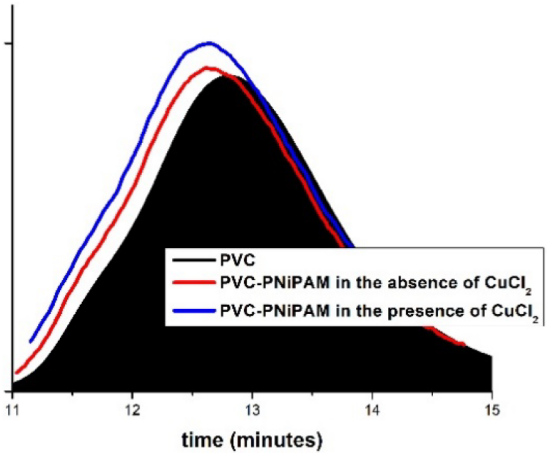

Figure 13. GPC traces for the poly(NIPAM) graft on the PVC surface.

and the molecular weights do not display a clear dependence on the conversion value (Figure 10).

The results confirm that the **polymerization evolution is strictly dependent on the nature of the solvent used and its interaction with Cu^{2+}ions** (as it can be observed from the images in Figure 11, the change in color signifying different

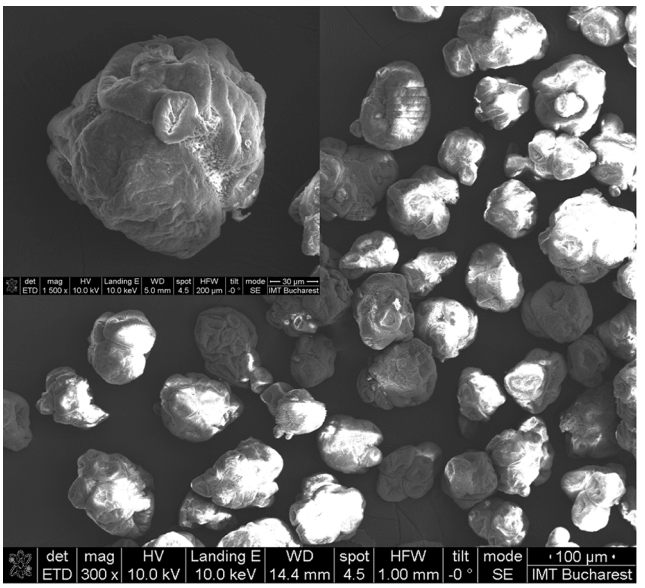

a)

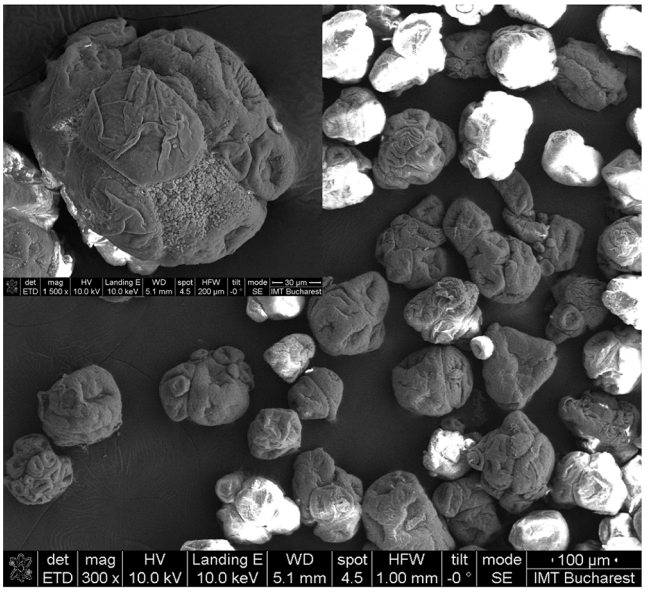

b)

Figure 14. SEM images of PVC (a) and PVC-*graft*-PNIPAM (b) (in the absence of $CuCl_2$).

coordination of Cu^{2+} ions). Thus, if the solvent facilitates the dissolution of Cu^{2+}, the SARA-ATRP mechanism is improved.

3.5. Synthesis of Block Copolymers by Chain Extension with MMA. As presented in previous studies,[40,73] if a polymerization follows a SARA-ATRP mechanism, due to the **termination reactions, there is the possibility of the loss of terminal reactive functionality**. For this reason, we selected a specimen that presented a bimodal molecular weight distribution obtained by polymerization at 70 °C ($\mathbf{Mn_2}$ = 434000 g/mol, $Đ$ = 1.27 and $\mathbf{Mn_1}$ = 66780 g/mol, $Đ$ = 1.47). After the polymerization reaction, through chain extension, a polymer with a bimodal molecular weight distribution was obtained with an increase of $\mathbf{Mn_2}$ = 510900 g/mol, $Đ$ = 1.12 while $\mathbf{Mn_1}$ remained unchanged at 66800 g/mol, $Đ$ = 1.47

https://doi.org/10.1021/acsomega.4c06179
ACS Omega 2024, 9, 42455−42469

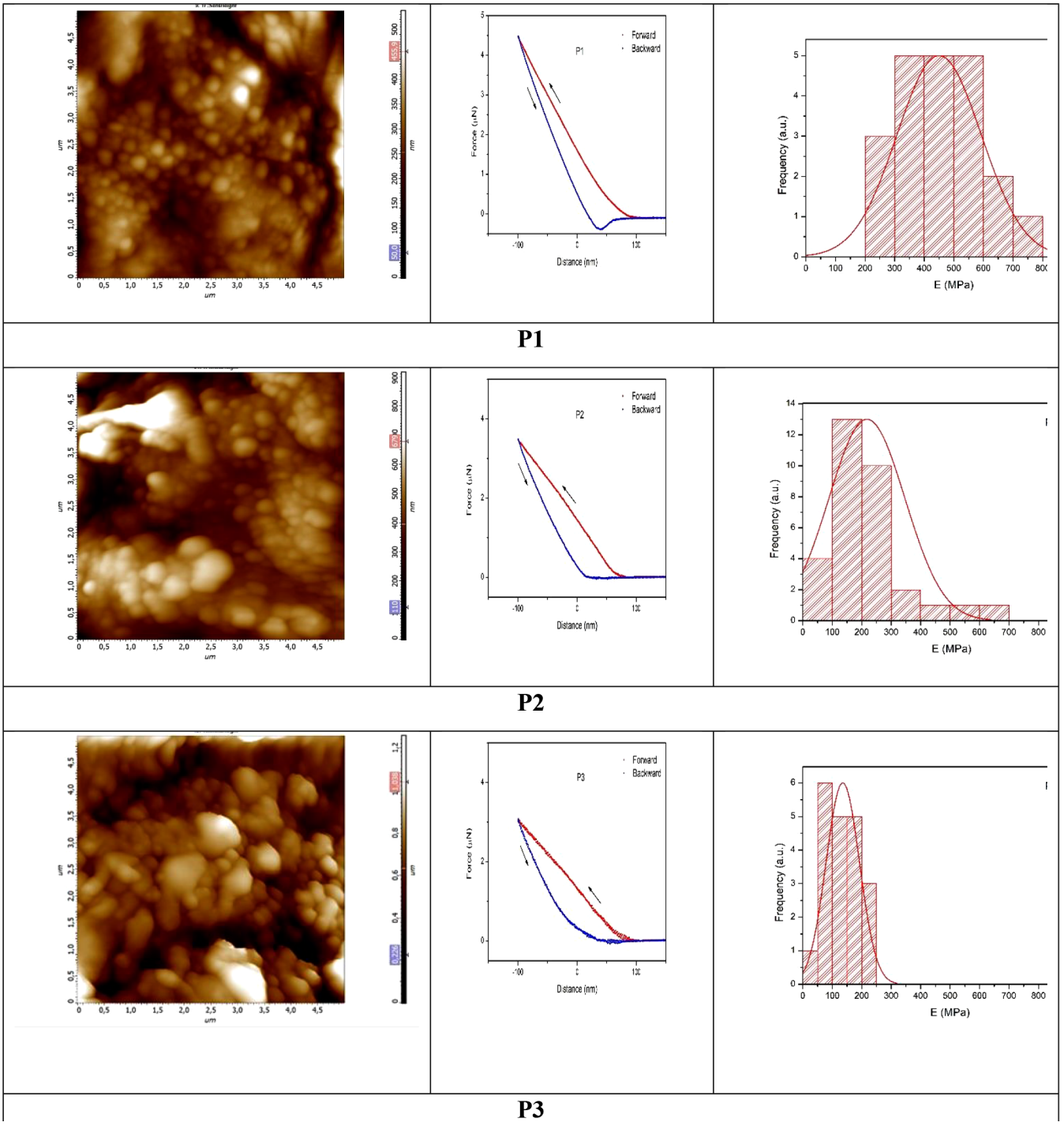

Figure 15. AFM images, representative force−distance curves, and histograms of Young's modulus for **P1, P2,** and **P3**.

(Figure 12), which sustains that the PMMA formation is the result of a SET-LRP mechanism.

In conclusion, the polymerization of MMA using PVC follows two types of mechanisms: one involving a SARA-ATRP process to generate the PMMA grafts onto the PVC backbone, which does not display a reactive terminal group capable of polymer extension, and a SET-LRP mechanism, which leads to the formation of a PMMA homopolymer, which retains the reactive terminal group.

3.6. Grafting PNIPAM on the PVC Surface. To further investigate the mechanism, we studied the influence of a polar and protic solvent (also "green"), such as water, to perform the grafting reaction. The reaction was performed at room temperature, using NIPAM as the monomer. The reaction involves surface-initiated (SI) grafting from the PVC suspension particles in the presence and the absence of $CuCl_2$ salt. The reaction was performed in the presence of a Cu^{2+} salt to shift the equilibrium toward the formation of additional Cu^{+} species.

After performing the polymerization reaction under the same conditions (4 h reaction time), the presence of Cu^{2+} salt led to the formation of an Mn_1 of 82200 g/mol with a dispersity (Đ) value of 1.67, which signifies almost a doubling of the molecular weight versus PVC, and the grafting in the

https://doi.org/10.1021/acsomega.4c06179
ACS Omega 2024, 9, 42455−42469

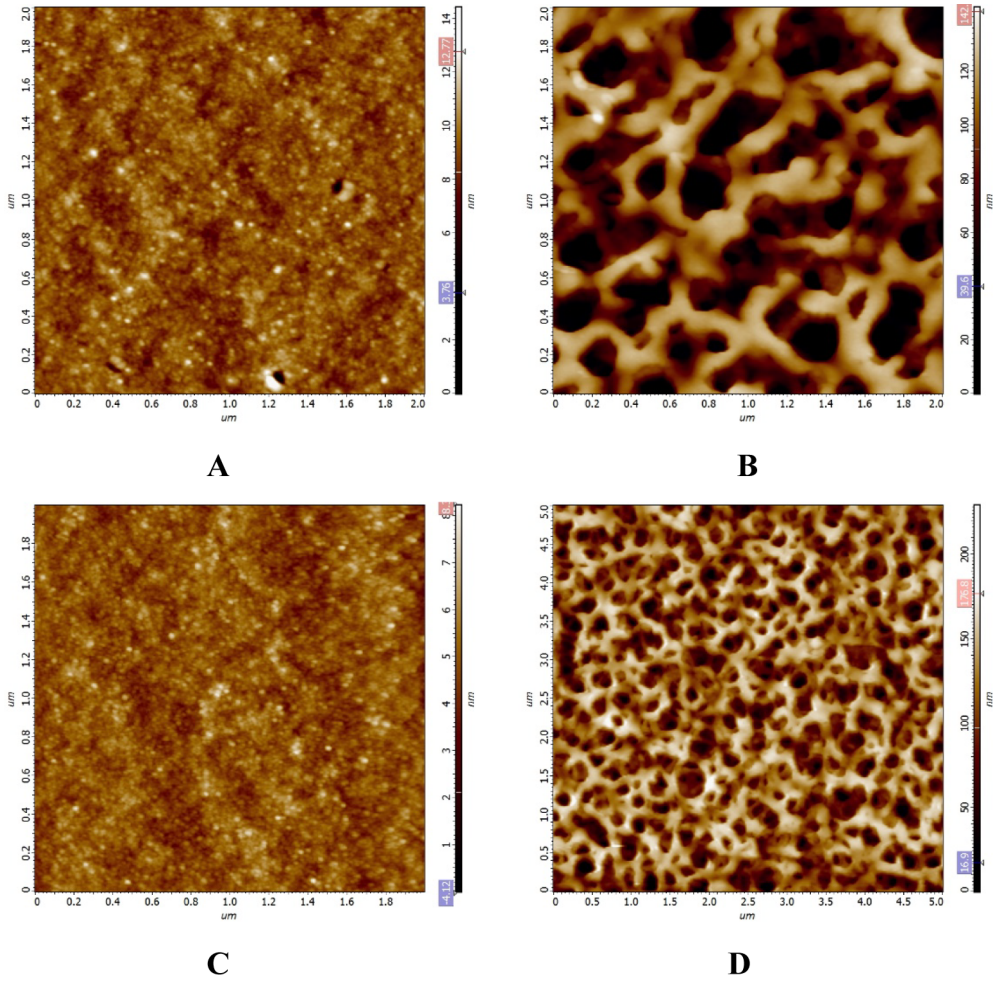

Figure 16. Surface morphologies for A) PVC-p(NIPAM) (in the absence of $CuCl_2$)−**P2**; B) PVC-p(NIPAM) (in the presence of $CuCl_2$)−**P3**; C) PVC (**P1**) and D) PVC-p(NIPAM) (in the presence of $CuCl_2$) (**P3**).

absence of a Cu^{2+}salt (Mn_1 of 63 700 g/mol and Đ = 1.95) was obtained (Figure 13). Thus, it can be noticed that in the presence of a Cu^{2+} salt, higher molecular weights are obtained with a narrower dispersity value. This aspect sustains the successful grafting of PMMA on the surface of PVC by a SARA-ATRP mechanism,[41,85,86] in the presence of metallic copper.[87,88]

The initial PVC- and PNIPAM-functionalized PVC particles (in the absence of $CuCl_2$) were characterized by SEM and EDX (Figure 14). It is easily observed that the initial dimension varies between 70 and 100 μm, while the ones functionalized with PNIPAM suffer a 10−20 μm size increase.

Figure 15 displays a typical topography image acquired for the reference sample (PVC) (P1), the sample modified with PNIPAM (in the absence of $CuCl_2$) (P2), and the sample modified with PNIPAM (in the presence of $CuCl_2$) (P3), together with representative force−distance curves and histograms of Young's modulus measured for each sample. The derived average elastic modulus values were E = 450 MPa (P1), 217 MPa (P2), and 136 MPa (P3). It is worth noting that for the case of core−shell particles, our approach provides a combined Young's modulus of the shell and of the underlying core.

Figure 16a−c presents the typical images of the surface morphologies at 2 μm by 2 μm scan size. Additionally, Figure 16d displays the morphology of P2 (PVC—poly(NIPAM) in the presence of $CuCl_2$) at 5 μm × 5 μm scan size.

One can see that the images for samples A (**P2**) and C (**P1**) are very similar, both exhibiting a fine-grained morphology, with a Z scale of a few nm and <1 nm rms roughness. The size of individual grains noticeable in the images, which comprises the film morphology, is ∼20 nm, on the order of the AFM tip dimensions. On the contrary, sample B (**P2** - PVC-poly-(NIPAM) (in the presence of $CuCl_2$) displays a very different morphology, resembling a macroporous nanostructure with pore sizes typically on the order of 150−250 nm and a wall thickness of about 100 nm, leading to a surface rms roughness of ∼30 nm. This structured honeycomb arrangement results from the interpenetration between the soft poly(NIPAM) and hard PVC polymers under the particular conditions of film formation (employed solvent, proportion of the two components, thermal treatment). An attempt to "scratch" the honeycomb walls revealed that the nanostructure walls consist of underlying strands comprised of particles tens of nanometers in size, wrapped in an amorphous shell about 15 nm thick.

4. CONCLUSIONS

This study presents for the first time in the literature the controlled polymerization of MMA in the presence of PVC using metallic Cu^0. Initially, the polymerizations were performed at 60 and 70 °C, in bulk, with the obtaining of

https://doi.org/10.1021/acsomega.4c06179
ACS Omega 2024, 9, 42455−42469

two different polymer species, one of the order **of the initial PVC (10^4 g/mol) and another of the order 10^6 g/mol**. The first species represents **PVC grafted with PMMA**, while the second species represents **PMMA resulting from chain transfer reactions with the monomer**. From the kinetics analyses, it was demonstrated that the grafting process follows a SARA-ATRP mechanism, while the homopolymerization involves a SET-LRP reaction mechanism, which was confirmed by subsequent chain extension reactions.

Unrelated to the debate over the mechanism, in practical applications, Cu^0 has several **key advantages** compared to other **RDRP**[40−48] methods, which include fast and ultrafast reaction rates at room temperature, a simple reaction system, high purity of the final polymer, which will contain only trace amounts of copper, nearly colorless products, tolerance to impurities and air, compatibility with a wide range of organic solvents and aqueous media. Also, the catalyst, a copper wire, can be easily removed from the system after polymerization and reused.

To investigate the influence of the solvent, respectively, of a Cu^{2+} salt on the evolution of the reactions, experiments using water as a solvent were performed. The addition of Cu^{2+} salt favors the poly(NIPAM) grafting reaction in water, as confirmed by GPC, SEM, and AFM analyses.

In conclusion, it was evidenced for the first time that the MMA polymerization in the presence of PVC and metallic copper involves two types of controlled polymerization reactions: one of PVC grafting by SARA-ATRP and a homopolymerization process of MMA by transfer with the monomer following the SET-LRP route.

■ ASSOCIATED CONTENT

Supporting Information

The Supporting Information is available free of charge at https://pubs.acs.org/doi/10.1021/acsomega.4c06179.

The ^{1}H RMN spectra for the PVC modified with PMMA (a) PVC-g-PMMA-1, reaction time 60 minutes; (b) PVC-g-PMMA-2, reaction time 120 minutes; PVC-g-PMMA-3, reaction time 180 minutes; DMA results a) PVC-graft-PMMA 1; = max loss modulus: 77°C, max tan delta: 83°C; b) PVC-graft-PMMA 2; = max loss modulus: 80°C, max tan delta: 86°C; c) PVC-graft-PMMA 3; = max loss modulus: 73° and 87°C , max tan delta: 77° and 89°C(PDF)

■ AUTHOR INFORMATION

Corresponding Author

Edina Rusen − *Faculty of Chemical Engineering and Biotechnologies, National University of Science and Technology Politehnica Bucharest, Bucharest 011061, Romania;* orcid.org/0000-0002-1660-017X; Email: edina_rusen@yahoo.com

Authors

Alexandra Mocanu − *Faculty of Chemical Engineering and Biotechnologies, National University of Science and Technology Politehnica Bucharest, Bucharest 011061, Romania; National Institute for Research and Development in Microtechnologies—IMT Bucharest, Bucharest 077190, Romania*

Oana Brincoveanu − *National Institute for Research and Development in Microtechnologies—IMT Bucharest, Bucharest 077190, Romania; Research Institute of the University of Bucharest, ICUB Bucharest, Bucureşti 050663, Romania*

Gabriela Toader − *Military Technical Academy "Ferdinand I", Bucharest 050141, Romania*

Raluca Gavrila − *National Institute for Research and Development in Microtechnologies—IMT Bucharest, Bucharest 077190, Romania*

Aurel Diacon − *Faculty of Chemical Engineering and Biotechnologies, National University of Science and Technology Politehnica Bucharest, Bucharest 011061, Romania; Military Technical Academy "Ferdinand I", Bucharest 050141, Romania*

Cristina Stavarache − *Advanced Polymer Materials Group, University Politehnica of Bucharest, Bucharest 011061, Romania; "C. D. Nenitzescu" Institute of Organic and Supramolecular Chemistry202-B Spl. Independentei, Bucharest 060023, Romania*

Complete contact information is available at: https://pubs.acs.org/10.1021/acsomega.4c06179

Notes

The authors declare no competing financial interest.

■ ACKNOWLEDGMENTS

This work was partially granted by the Ministry of National Education (by UEFISCDI) through the national research projects PN−III-P2-2.1-PTE-2021-0514−contract 80PTE/2022. Aurel Diacon gratefully acknowledges financial support from the Competitiveness Operational Program 2014−2020, Action 1.1.3: Creating synergies with RDI actions of the EU's HORIZON 2020 framework program and other international RDI programs, MySMIS Code 108792, Acronym project "UPB4H", financed by contract: 250/11.05.2020.

■ REFERENCES

(1) Endo, K. Synthesis and structure of poly(vinyl chloride). *Prog. Polym. Sci.* **2002**, *27* (10), 2021−2054.

(2) Çoşkun, M.; Seven, P. Synthesis, characterization and investigation of dielectric properties of two-armed graft copolymers prepared with methyl methacrylate and styrene onto PVC using atom transfer radical polymerization. *React. Funct. Polym.* **2011**, *71* (4), 395−401.

(3) Suzuki, T. Chemical modification of PVC. *Pure Appl. Chem.* **1977**, *49* (5), 539−567.

(4) Kameda, T.; Ono, M.; Grause, G.; Mizoguchi, T.; Yoshioka, T. Chemical modification of poly(vinyl chloride) by nucleophilic substitution. *Polym. Degrad. Stab.* **2009**, *94* (1), 107−112.

(5) Krys, P.; Matyjaszewski, K. Kinetics of Atom Transfer Radical Polymerization. *Eur. Polym. J.* **2017**, *89*, 482−523.

(6) Parkatzidis, K.; Wang, H. S.; Truong, N. P.; Anastasaki, A. Recent Developments and Future Challenges in Controlled Radical Polymerization: A 2020 Update. *Chem* **2020**, *6* (7), 1575−1588.

(7) Matyjaszewski, K.; Spanswick, J. Controlled/living radical polymerization. *Mater. Today* **2005**, *8* (3), 26−33.

(8) Corrigan, N.; Jung, K.; Moad, G.; Hawker, C. J.; Matyjaszewski, K.; Boyer, C. Reversible-deactivation radical polymerization (Controlled/living radical polymerization): From discovery to materials design and applications. *Prog. Polym. Sci.* **2020**, *111*, 101311.

(9) Lamontagne, H. R.; Lessard, B. H. Nitroxide-Mediated Polymerization: A Versatile Tool for the Engineering of Next Generation Materials. *ACS Appl. Polym. Mater.* **2020**, *2* (12), 5327−5344.

(10) Maric, M. Application of Nitroxide Mediated Polymerization in Different Monomer Systems. *Curr. Org. Chem.* **2018**, *22* (13), 1264−1284.
(11) Perrier, S. 50th Anniversary Perspective: RAFT Polymerization—A User Guide. *Macromolecules* **2017**, *50* (19), 7433−7447.
(12) Boyer, C.; Bulmus, V.; Davis, T. P.; Ladmiral, V.; Liu, J.; Perrier, S. Bioapplications of RAFT Polymerization. *Chem. Rev.* **2009**, *109* (11), 5402−5436.
(13) Matyjaszewski, K.; Xia, J. Atom Transfer Radical Polymerization. *Chem. Rev.* **2001**, *101* (9), 2921−2990.
(14) Matyjaszewski, K. Atom Transfer Radical Polymerization (ATRP): Current Status and Future Perspectives. *Macromolecules* **2012**, *45* (10), 4015−4039.
(15) Lorandi, F.; Fantin, M.; Matyjaszewski, K. Atom Transfer Radical Polymerization: A Mechanistic Perspective. *J. Am. Chem. Soc.* **2022**, *144* (34), 15413−15430.
(16) Huang, Z.; Feng, C.; Guo, H.; Huang, X. Direct functionalization of poly(vinyl chloride) by photo-mediated ATRP without a deoxygenation procedure. *Polym. Chem.* **2016**, *7* (17), 3034−3045.
(17) Rusen, E.; ¸omoghi, R.; Busuioc, C.; Diacon, A. Hydrophilic modification of polyvinyl chloride with polyacrylic acid using ATRP. *RSC Adv.* **2020**, *10* (59), 35692−35700.
(18) Fahmy, A.; Abu Saied, M. A.; Morgan, N.; Qutop, W.; Abdelbary, H.; El-Bahy, S. M.; Schönhals, A.; Friedrich, J. F. Modified polyvinyl chloride membrane grafted with an ultra-thin polystyrene film: Structure and electrochemical properties. *J. Mater. Res. Technol.* **2021**, *12*, 2273−2284.
(19) Pan, X.; Fantin, M.; Yuan, F.; Matyjaszewski, K. Externally controlled atom transfer radical polymerization. *Chem. Soc. Rev.* **2018**, *47* (14), 5457−5490.
(20) Gao, H.; Matyjaszewski, K. Synthesis of Star Polymers by a Combination of ATRP and the "Click" Coupling Method. *Macromolecules* **2006**, *39* (15), 4960−4965.
(21) Patten, T. E.; Xia, J.; Abernathy, T.; Matyjaszewski, K. Polymers with Very Low Polydispersities from Atom Transfer Radical Polymerization. *Science* **1996**, *272* (5263), 866−868.
(22) Brown, S.; Chatterjee, S.; Li, M.; Yue, Y.; Tsouris, C.; Janke, C. J.; Saito, T.; Dai, S. Uranium Adsorbent Fibers Prepared by Atom-Transfer Radical Polymerization from Chlorinated Polypropylene and Polyethylene Trunk Fibers. *Ind. Eng. Chem. Res.* **2016**, *55* (15), 4130−4138.
(23) Ahmad, T.; Liu, X.; Guria, C. Preparation of polyvinyl chloride (PVC) membrane blended with acrylamide grafted bentonite for oily water treatment. *Chemosphere* **2023**, *310*, 136840.
(24) Zou, Y.; Kizhakkedathu, J. N.; Brooks, D. E. Surface Modification of Polyvinyl Chloride Sheets via Growth of Hydrophilic Polymer Brushes. *Macromolecules* **2009**, *42* (9), 3258−3268.
(25) Mohammad, S. A.; Shingdilwar, S.; Banerjee, S. Recoverable and recyclable nickel−cobalt magnetic alloy nanoparticle catalyzed reversible deactivation radical polymerization of methyl methacrylate at 25 °C. *Polym. Chem.* **2020**, *11* (2), 287−291.
(26) Góis, J. R.; Konkolewic, D.; Popov, A. V.; Guliashvili, T.; Matyjaszewski, K.; Serra, A. C.; Coelho, J. F. J. Improvement of the control over SARA ATRP of 2-(diisopropylamino)ethyl methacrylate by slow and continuous addition of sodium dithionite. *Polym. Chem.* **2014**, *5* (16), 4617−4626.
(27) Gao, Y.; Zhao, T.; Wang, W. Is it ATRP or SET-LRP? part I: Cu0&CuII/PMDETA - mediated reversible - deactivation radical polymerization. *RSC Adv.* **2014**, *4* (106), 61687−61690.
(28) Visnevskij, C.; Makuska, R. SARA ATRP in Aqueous Solutions Containing Supplemental Redox Intermediate: Controlled Polymerization of [2-(Methacryloyloxy)ethyl] trimethylammonium Chloride. *Macromolecules* **2013**, *46* (12), 4764−4771.
(29) Abreu, C. M. R.; Fu, L.; Carmali, S.; Serra, A. C.; Matyjaszewski, K.; Coelho, J. F. J. Aqueous SARA ATRP using inorganic sulfites. *Polym. Chem.* **2017**, *8* (2), 375−387.
(30) Krys, P.; Wang, Y.; Matyjaszewski, K.; Harrisson, S. Radical Generation and Termination in SARA ATRP of Methyl Acrylate: Effect of Solvent, Ligand, and Chain Length. *Macromolecules* **2016**, *49* (8), 2977−2984.
(31) Dadashi-Silab, S.; Matyjaszewski, K. Temporal Control in Atom Transfer Radical Polymerization Using Zerovalent Metals. *Macromolecules* **2018**, *51* (11), 4250−4258.
(32) Anastasaki, A.; Nikolaou, V.; Haddleton, D. M. Cu(0)-mediated living radical polymerization: Recent highlights and applications; a perspective. *Polym. Chem.* **2016**, *7* (5), 1002−1026.
(33) Levere, M. E.; Nguyen, N. H.; Leng, X.; Percec, V. Visualization of the crucial step in SET-LRP. *Polym. Chem.* **2013**, *4* (5), 1635−1647.
(34) Lligadas, G.; Grama, S.; Percec, V. Single-Electron Transfer Living Radical Polymerization Platform to Practice, Develop, and Invent. *Biomacromolecules* **2017**, *18* (10), 2981−3008.
(35) Levere, M. E.; Willoughby, I.; O'Donohue, S.; de Cuendias, A.; Grice, A. J.; Fidge, C.; Becer, C. R.; Haddleton, D. M. Assessment of SET-LRP in DMSO using online monitoring and Rapid GPC. *Polym. Chem.* **2010**, *1* (7), 1086−1094.
(36) Samanta, S. R.; Cai, R.; Percec, V. SET-LRP of semifluorinated acrylates and methacrylates. *Polym. Chem.* **2014**, *5* (18), 5479−5491.
(37) Anastasaki, A.; Nikolaou, V.; Nurumbetov, G.; Wilson, P.; Kempe, K.; Quinn, J. F.; Davis, T. P.; Whittaker, M. R.; Haddleton, D. M. Cu(0)-Mediated Living Radical Polymerization: A Versatile Tool for Materials Synthesis. *Chem. Rev.* **2016**, *116* (3), 835−877.
(38) Boyer, C.; Corrigan, N. A.; Jung, K.; Nguyen, D.; Nguyen, T.-K.; Adnan, N. N. M.; Oliver, S.; Shanmugam, S.; Yeow, J. Copper-Mediated Living Radical Polymerization (Atom Transfer Radical Polymerization and Copper(0) Mediated Polymerization): From Fundamentals to Bioapplications. *Chem. Rev.* **2016**, *116* (4), 1803−1949.
(39) Enayati, M.; Abbaspourrad, A. Cu(0)-mediated reversible-deactivation radical polymerization of n-butyl acrylate in suspension. *Polymer* **2018**, *153*, 464−473.
(40) Konkolewicz, D.; Krys, P.; Góis, J. R.; Mendonça, P. V.; Zhong, M.; Wang, Y.; Gennaro, A.; Isse, A. A.; Fantin, M.; Matyjaszewski, K. Aqueous RDRP in the Presence of Cu0: The Exceptional Activity of CuI Confirms the SARA ATRP Mechanism. *Macromolecules* **2014**, *47* (2), 560−570.
(41) Konkolewicz, D.; Wang, Y.; Krys, P.; Zhong, M.; Isse, A. A.; Gennaro, A.; Matyjaszewski, K. SARA ATRP or SET-LRP. End of controversy? *Polym. Chem.* **2014**, *5* (15), 4396−4417.
(42) Lyu, J.; Miao, Y.; Li, Z.; Li, Y.; Gao, Y.; Johnson, M.; Tai, H.; Wang, W. Where is the induction from? Effect of disproportionation and comproportionation in Cu(0)-mediated reversible deactivation radical polymerization. *Polymer* **2023**, *280*, 126055.
(43) Diacon, A.; Rusen, E.; Rizea, F.; Ghebaur, A.; Berger, D.; Somoghi, R.; Matei, A.; Palade, P.; Tutunaru, O. One-pot strategy for obtaining magnetic PMMA particles through ATRP using Fe(CO)5 as co-initiator. *Eur. Polym. J.* **2021**, *152*, 110446.
(44) Rusen, E.; Somoghi, R.; Busuioc, C.; Diacon, A. Hydrophilic modification of polyvinyl chloride with polyacrylic acid using ATRP. *RSC Adv.* **2020**, *10* (59), 35692−35700.
(45) Rusen, E.; Diacon, A.; Mocanu, A.; Culita, D. C.; Dinescu, A.; Zecheru, T. "A real" emulsion polymerization using simple ATRP reaction in the presence of an oligo-initiator with a dual activity of emulsifier and initiator. *Colloids Surf., A* **2018**, *555*, 1−7.
(46) Rusen, E.; Mocanu, A. Atom transfer radical emulsion polymerization (emulsion ATRP) of styrene with water-soluble initiator. *Colloid Polym. Sci.* **2013**, *291* (9), 2253−2257.
(47) Diacon, A.; Rusen, E.; Mocanu, A.; Nistor, L. C. Supported Cu^0 nanoparticles catalyst for controlled radical polymerization reaction and block-copolymer synthesis. *Sci. Rep.* **2017**, *7* (1), 10345.
(48) Whitfield, R.; Anastasaki, A.; Jones, G. R.; Haddleton, D. M. Cu(0)-RDRP of styrene: Balancing initiator efficiency and dispersity. *Polym. Chem.* **2018**, *9*, 4395−4403.
(49) Percec, V.; Guliashvili, T.; Ladislaw, J. S.; Wistrand, A.; Stjerndahl, A.; Sienkowska, M. J.; Monteiro, M. J.; Sahoo, S. Ultrafast Synthesis of Ultrahigh Molar Mass Polymers by Metal-Catalyzed Living Radical Polymerization of Acrylates, Methacrylates, and Vinyl

https://doi.org/10.1021/acsomega.4c06179
ACS Omega 2024, 9, 42455−42469

Chloride Mediated by SET at 25 °C. *J. Am. Chem. Soc.* **2006**, *128* (43), 14156−14165.
(50) Enayati, M.; Jezorek, R. L.; Monteiro, M. J.; Percec, V. Ultrafast SET-LRP of hydrophobic acrylates in multiphase alcohol-water mixtures. *Polym. Chem.* **2016**, *7* (21), 3608−3621.
(51) Sundaram, H. S.; Raghavachari, D. Controlled radical polymerization of tert-butyl acrylate at ambient temperature: Effect of initiator structure and synthesis of amphiphilic block copolymers. *J. Polym. Sci., Part A: Polym. Chem.* **2012**, *50* (5), 996−1007.
(52) Mosnáček, J.; Ilčíková, M. Photochemically Mediated Atom Transfer Radical Polymerization of Methyl Methacrylate Using ppm Amounts of Catalyst. *Macromolecules* **2012**, *45* (15), 5859−5865.
(53) Enayati, M.; Smail, R. B.; Grama, S.; Jezorek, R. L.; Monteiro, M. J.; Percec, V. The synergistic effect during biphasic SET-LRP in ethanol−nonpolar solvent−water mixtures. *Polym. Chem.* **2016**, *7* (47), 7230−7241.
(54) Waldron, C.; Zhang, Q.; Li, Z.; Nikolaou, V.; Nurumbetov, G.; Godfrey, J.; McHale, R.; Yilmaz, G.; Randev, R. K.; Girault, M.; McEwan, K.; Haddleton, D. M.; Droesbeke, M.; Haddleton, A. J.; Wilson, P.; Simula, A.; Collins, J.; Lloyd, D. J.; Burns, J. A.; Summers, C.; Houben, C.; Anastasaki, A.; Li, M.; Becer, C. R.; Kiviaho, J. K.; Risangud, N. Absolut "copper catalyzation perfected"; robust living polymerization of NIPAM: Guinness is good for SET-LRP. *Polym. Chem.* **2014**, *5* (1), 57−61.
(55) Flejszar, M.; Chmielarz, P.; Oszajca, M. Red is the new green: Dry wine-based miniemulsion as eco-friendly reaction medium for sustainable atom transfer radical polymerization. *J. Appl. Polym. Sci.* **2023**, *140* (7), No. e53367.
(56) Bensabeh, N.; Moreno, A.; Maurya, D. S.; Adamson, J.; Galià, M.; Lligadas, G.; Percec, V. Resolving the incompatibility between SET-LRP and non-disproportionating solvents. *Giant* **2023**, *15*, 100176.
(57) Grama, S.; Lejnieks, J.; Enayati, M.; Smail, R. B.; Ding, L.; Lligadas, G.; Monteiro, M. J.; Percec, V. Searching for efficient SET-LRP systems via biphasic mixtures of water with carbonates, ethers and dipolar aprotic solvents. *Polym. Chem.* **2017**, *8* (38), 5865−5874.
(58) Zhang, Q.; Wilson, P.; Li, Z.; McHale, R.; Godfrey, J.; Anastasaki, A.; Waldron, C.; Haddleton, D. M. Aqueous Copper-Mediated Living Polymerization: Exploiting Rapid Disproportionation of CuBr with Me6TREN. *J. Am. Chem. Soc.* **2013**, *135* (19), 7355−7363.
(59) Dworakowska, S.; Lorandi, F.; Gorczyński, A.; Matyjaszewski, K. Toward Green Atom Transfer Radical Polymerization: Current Status and Future Challenges. *Adv. Sci.* **2022**, *9* (19), 2106076.
(60) Flejszar, M.; ́lusarczyk, K.; Hochół, A.; Chmielarz, P.; Spilarewicz, K.; Błoniarz, P. Replacing organics with water: Macromolecular engineering of non-water miscible poly(meth)acrylates via interfacial and ion-pair catalysis SARA ATRP in miniemulsion. *Eur. Polym. J.* **2023**, *197*, 112374.
(61) Zaborniak, I.; Chmielarz, P.; Wolski, K. Riboflavin-induced metal-free ATRP of (meth)acrylates. *Eur. Polym. J.* **2020**, *140*, 110055.
(62) El Achi, N.; Bakkour, Y.; Adhami, W.; Molina, J.; Penhoat, M.; Azaroual, N.; Chausset-Boissarie, L.; Rolando, C. Metal-Free ATRP Catalyzed by Visible Light in Continuous Flow. *Front. Chem.* **2020**, *8*, 740.
(63) Corrigan, N.; Zhernakov, L.; Hashim, M. H.; Xu, J.; Boyer, C. Flow mediated metal-free PET-RAFT polymerisation for upscaled and consistent polymer production. *React. Chem. Eng.* **2019**, *4* (7), 1216−1228.
(64) Zhang, T.; Yeow, J.; Boyer, C. A cocktail of vitamins for aqueous RAFT polymerization in an open-to-air microtiter plate. *Polym. Chem.* **2019**, *10* (34), 4643−4654.
(65) Allushi, A.; Jockusch, S.; Yilmaz, G.; Yagci, Y. Photoinitiated Metal-Free Controlled/Living Radical Polymerization Using Polynuclear Aromatic Hydrocarbons. *Macromolecules* **2016**, *49* (20), 7785−7792.
(66) Miyake, G. M.; Theriot, J. C. Perylene as an Organic Photocatalyst for the Radical Polymerization of Functionalized Vinyl Monomers through Oxidative Quenching with Alkyl Bromides and Visible Light. *Macromolecules* **2014**, *47* (23), 8255−8261.
(67) Park, G. S.; Back, J.; Choi, E. M.; Lee, E.; Son, K.-S. Visible light-mediated metal-free atom transfer radical polymerization with N-trifluoromethylphenyl phenoxazines. *Eur. Polym. J.* **2019**, *117*, 347−352.
(68) Leggat, P. A.; Smith, D. R.; Kedjarune, U. Surgical Applications of Methyl Methacrylate: A Review of Toxicity. *Arch. Environ. Occup. Health* **2009**, *64* (3), 207−212.
(69) Martinez, M. R.; Schild, D.; De Luca Bossa, F.; Matyjaszewski, K. Depolymerization of Polymethacrylates by Iron ATRP. *Macromolecules* **2022**, *55* (23), 10590−10599.
(70) Lu, L.; Li, W.; Cheng, Y.; Liu, M. Chemical recycling technologies for PVC waste and PVC-containing plastic waste: A review. *Waste Manage.* **2023**, *166*, 245−258.
(71) Jiang, X.; Zhu, B.; Zhu, M. An overview on the recycling of waste poly(vinyl chloride). *Green Chem.* **2023**, *25* (18), 6971−7025.
(72) Gavrilov, M.; Monteiro, M. J. Derivation of the molecular weight distributions from size exclusion chromatography. *Eur. Polym. J.* **2015**, *65*, 191−196.
(73) Liarou, E.; Whitfield, R.; Anastasaki, A.; Engelis, N. G.; Jones, G. R.; Velonia, K.; Haddleton, D. M. Copper-Mediated Polymerization without External Deoxygenation or Oxygen Scavengers. *Angew. Chem., Int. Ed.* **2018**, *57* (29), 8998−9002.
(74) Matyjaszewski, K. Atom Transfer Radical Polymerization (ATRP): Current Status and Future Perspectives. *Macromolecules* **2012**, *45*, 4015−4039.
(75) Matyjaszewski, K. Advanced Materials by Atom Transfer Radical Polymerization. *Adv. Mater.* **2018**, *30* (23), 1706441.
(76) Matyjaszewski, K.; Patten, T. E.; Xia, J. Controlled/"Living" Radical Polymerization. Kinetics of the Homogeneous Atom Transfer Radical Polymerization of Styrene. *J. Am. Chem. Soc.* **1997**, *119* (4), 674−680.
(77) Tang, W.; Kwak, Y.; Braunecker, W.; Tsarevsky, N. V.; Coote, M. L.; Matyjaszewski, K. Understanding Atom Transfer Radical Polymerization: Effect of Ligand and Initiator Structures on the Equilibrium Constants. *J. Am. Chem. Soc.* **2008**, *130* (32), 10702−10713.
(78) Moreno, A.; Bensabeh, N.; Parve, J.; Ronda, J. C.; Cádiz, V.; Galià, M.; Vares, L.; Lligadas, G.; Percec, V. SET-LRP of Bio- and Petroleum-Sourced Methacrylates in Aqueous Alcoholic Mixtures. *Biomacromolecules* **2019**, *20* (4), 1816−1827.
(79) Chmielarz, P.; Krys, P.; Park, S.; Matyjaszewski, K. PEO-b-PNIPAM copolymers via SARA ATRP and eATRP in aqueous media. *Polymer* **2015**, *71*, 143−147.
(80) Rabea, A. M.; Zhu, S. Modeling the Influence of Diffusion-Controlled Reactions and Residual Termination and Deactivation on the Rate and Control of Bulk ATRP at High Conversions. *Polymers* **2015**, *7* (5), 819−835.
(81) Huang, Z.; Feng, C.; Guo, H.; Huang, X. Direct functionalization of poly(vinyl chloride) by photo-mediated ATRP without a deoxygenation procedure11Electronic supplementary information (ESI) available See. *Polym. Chem.* **2016**, *7* (17), 3034−3045.
(82) Sugumaran, D.; Karim, K. Removal of copper (II) ion using chitosan-graft-poly (methyl methacrylate) as adsorbent. *Eproc. Chem.* **2017**, *2* (1), 1−11.
(83) Maaz, M.; Elzein, T.; Bejjani, A.; Barroca-Aubry, N.; Lepoittevin, B.; Dragoe, D.; Mazerat, S.; Nsouli, B.; Roger, P. Surface initiated supplemental activator and reducing agent atom transfer radical polymerization (SI-SARA-ATRP) of 4-vinylpyridine on poly(ethylene terephthalate). *J. Colloid Interface Sci.* **2017**, *500*, 69−78.
(84) Konkolewicz, D.; Wang, Y.; Zhong, M.; Krys, P.; Isse, A. A.; Gennaro, A.; Matyjaszewski, K. Reversible-Deactivation Radical Polymerization in the Presence of Metallic Copper. A Critical Assessment of the SARA ATRP and SET-LRP Mechanisms. *Macromolecules* **2013**, *46* (22), 8749−8772.

https://doi.org/10.1021/acsomega.4c06179
ACS Omega 2024, 9, 42455−42469

(85) Magenau, A. J. D.; Kwak, Y.; Matyjaszewski, K. ATRP of Methacrylates Utilizing CuIIX2/L and Copper Wire. *Macromolecules* **2010**, *43* (23), 9682−9689.
(86) Alsubaie, F.; Anastasaki, A.; Nikolaou, V.; Simula, A.; Nurumbetov, G.; Wilson, P.; Kempe, K.; Haddleton, D. M. Investigating the Mechanism of Copper(0)-Mediated Living Radical Polymerization in Aqueous Media. *Macromolecules* **2015**, *48* (18), 6421−6432.
(87) Yang, Y.; Wang, J.; Wu, F.; Ye, G.; Yi, R.; Lu, Y.; Chen, J. Surface-initiated SET-LRP mediated by mussel-inspired polydopamine chemistry for controlled building of novel core−shell magnetic nanoparticles for highly-efficient uranium enrichment. *Polym. Chem.* **2016**, *7* (13), 2427−2435.
(88) Zoppe, J. O.; Ataman, N. C.; Mocny, P.; Wang, J.; Moraes, J.; Klok, H.-A. Surface-Initiated Controlled Radical Polymerization: State-of-the-Art, Opportunities, and Challenges in Surface and Interface Engineering with Polymer Brushes. *Chem. Rev.* **2017**, *117* (3), 1105−1318.

https://doi.org/10.1021/acsomega.4c06179
ACS Omega 2024, 9, 42455−42469